

Today's outline - October 02, 2024





- Information about:
 - (a) Final presentation
 - (b) Final project

Today's outline - October 02, 2024



- Information about:
 - (a) Final presentation
 - (b) Final project
- Porod analysis

Today's outline - October 02, 2024



- Information about:
 - (a) Final presentation
 - (b) Final project
- Porod analysis
- SAXS papers



- Information about:
 - (a) Final presentation
 - (b) Final project
- Porod analysis
- SAXS papers

Reading Assignment: Chapter 5.2–5.3

Today's outline - October 02, 2024



- Information about:
 - (a) Final presentation
 - (b) Final project
- Porod analysis
- SAXS papers

Reading Assignment: Chapter 5.2–5.3

Homework Assignment #03:

Chapter 3: 1,3,4,6,8

due Friday, October 05, 2024



- Information about:
 - (a) Final presentation
 - (b) Final project
- Porod analysis
- SAXS papers

Reading Assignment: Chapter 5.2–5.3

Homework Assignment #03:

Chapter 3: 1,3,4,6,8

due Friday, October 05, 2024

Homework Assignment #04:

Chapter 4: 2,4,6,7,10

due Monday, October 14, 2024



1. Choose paper for presentation



1. Choose paper for presentation
2. Clear it with me!



1. Choose paper for presentation
2. Clear it with me!
3. Do some background research on the technique



1. Choose paper for presentation
2. Clear it with me!
3. Do some background research on the technique
4. Prepare a 15 minute presentation



1. Choose paper for presentation
2. Clear it with me!
3. Do some background research on the technique
4. Prepare a 15 minute presentation
5. Be ready for questions!



1. Come up with a potential experiment



1. Come up with a potential experiment
2. Make sure it is a different technique than your final presentation

Final project



1. Come up with a potential experiment
2. Make sure it is a different technique than your final presentation
3. Clear it with me!



1. Come up with a potential experiment
2. Make sure it is a different technique than your final presentation
3. Clear it with me!
4. Find appropriate beamline(s) and if needed contact the beamline scientists (they are used to it)



1. Come up with a potential experiment
2. Make sure it is a different technique than your final presentation
3. Clear it with me!
4. Find appropriate beamline(s) and if needed contact the beamline scientists (they are used to it)
5. Lay out proposed experiment (you can ask for help!)



1. Come up with a potential experiment
2. Make sure it is a different technique than your final presentation
3. Clear it with me!
4. Find appropriate beamline(s) and if needed contact the beamline scientists (they are used to it)
5. Lay out proposed experiment (you can ask for help!)
6. Make sure to give reasonable answers for all the questions



1. Come up with a potential experiment
2. Make sure it is a different technique than your final presentation
3. Clear it with me!
4. Find appropriate beamline(s) and if needed contact the beamline scientists (they are used to it)
5. Lay out proposed experiment (you can ask for help!)
6. Make sure to give reasonable answers for all the questions
7. Put me as one of the investigators of the proposal

SAXS review



The SAXS scattered intensity from a dilute solution depends on the single particle form factor, $\mathcal{F}(\vec{Q})$, the volume of the particle, V_p , and the density difference from the solvent, $\Delta\rho = (\rho_{sl,p} - \rho_{sl,0})$

SAXS review



The SAXS scattered intensity from a dilute solution depends on the single particle form factor, $\mathcal{F}(\vec{Q})$, the volume of the particle, V_p , and the density difference from the solvent, $\Delta\rho = (\rho_{sl,p} - \rho_{sl,0})$

$$I^{SAXS}(\vec{Q}) = \Delta\rho^2 V_p^2 |\mathcal{F}(\vec{Q})|^2$$



The SAXS scattered intensity from a dilute solution depends on the single particle form factor, $\mathcal{F}(\vec{Q})$, the volume of the particle, V_p , and the density difference from the solvent, $\Delta\rho = (\rho_{sl,p} - \rho_{sl,0})$

$$I^{SAXS}(\vec{Q}) = \Delta\rho^2 V_p^2 |\mathcal{F}(\vec{Q})|^2$$

the long wavelength limit ($QR \rightarrow 0$) is called the Guinier regime and it is possible to extract the radius of gyration R_g of the particle



The SAXS scattered intensity from a dilute solution depends on the single particle form factor, $\mathcal{F}(\vec{Q})$, the volume of the particle, V_p , and the density difference from the solvent, $\Delta\rho = (\rho_{sl,p} - \rho_{sl,0})$

$$I^{SAXS}(\vec{Q}) = \Delta\rho^2 V_p^2 |\mathcal{F}(\vec{Q})|^2$$

$$I^{SAXS}(Q) \approx \Delta\rho^2 V_p^2 e^{-Q^2 R_g^2/3}$$

the long wavelength limit ($QR \rightarrow 0$) is called the Guinier regime and it is possible to extract the radius of gyration R_g of the particle

SAXS review

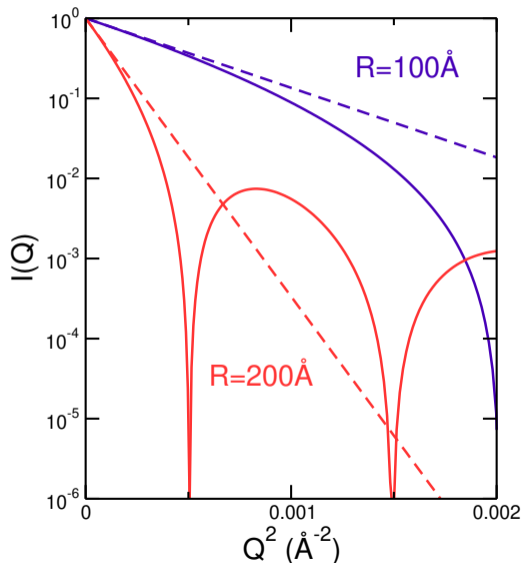


The SAXS scattered intensity from a dilute solution depends on the single particle form factor, $\mathcal{F}(\vec{Q})$, the volume of the particle, V_p , and the density difference from the solvent, $\Delta\rho = (\rho_{sl,p} - \rho_{sl,0})$

$$I^{SAXS}(\vec{Q}) = \Delta\rho^2 V_p^2 |\mathcal{F}(\vec{Q})|^2$$

$$I^{SAXS}(Q) \approx \Delta\rho^2 V_p^2 e^{-Q^2 R_g^2/3}$$

the long wavelength limit ($QR \rightarrow 0$) is called the Guinier regime and it is possible to extract the radius of gyration R_g of the particle





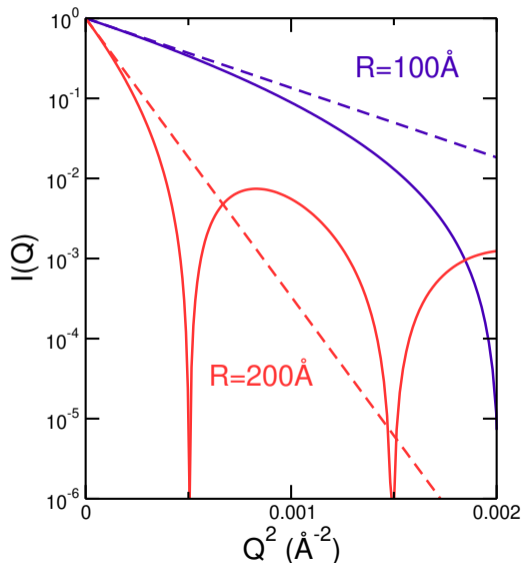
The SAXS scattered intensity from a dilute solution depends on the single particle form factor, $\mathcal{F}(\vec{Q})$, the volume of the particle, V_p , and the density difference from the solvent, $\Delta\rho = (\rho_{sl,p} - \rho_{sl,0})$

$$I^{SAXS}(\vec{Q}) = \Delta\rho^2 V_p^2 |\mathcal{F}(\vec{Q})|^2$$

$$I^{SAXS}(Q) \approx \Delta\rho^2 V_p^2 e^{-Q^2 R_g^2/3}$$

the long wavelength limit ($QR \rightarrow 0$) is called the Guinier regime and it is possible to extract the radius of gyration R_g of the particle

$$R_g^2 = \frac{\int_{V_p} \rho_{sl,p}(\vec{r}) r^2 dV_p}{\int_{V_p} \rho_{sl,p}(\vec{r}) dV_p}$$



Porod analysis



In the short wavelength limit ($QR \gg 1$), the form factor for a sphere can be approximated

Porod analysis



In the short wavelength limit ($QR \gg 1$), the form factor for a sphere can be approximated

$$\mathcal{F}(Q) = 3 \left[\frac{\sin(QR)}{Q^3 R^3} - \frac{\cos(QR)}{Q^2 R^2} \right]$$

Porod analysis



In the short wavelength limit ($QR \gg 1$), the form factor for a sphere can be approximated

$$\mathcal{F}(Q) = 3 \left[\frac{\sin(QR)}{Q^3 R^3} - \frac{\cos(QR)}{Q^2 R^2} \right] \approx 3 \left[-\frac{\cos(QR)}{Q^2 R^2} \right]$$

Porod analysis



In the short wavelength limit ($QR \gg 1$), the form factor for a sphere can be approximated

$$\mathcal{F}(Q) = 3 \left[\frac{\sin(QR)}{Q^3 R^3} - \frac{\cos(QR)}{Q^2 R^2} \right] \approx 3 \left[-\frac{\cos(QR)}{Q^2 R^2} \right]$$

$$I(Q) = 9\Delta\rho^2 V_p^2 \left[-\frac{\cos(QR)}{Q^2 R^2} \right]^2$$

Porod analysis



In the short wavelength limit ($QR \gg 1$), the form factor for a sphere can be approximated

$$\mathcal{F}(Q) = 3 \left[\frac{\sin(QR)}{Q^3 R^3} - \frac{\cos(QR)}{Q^2 R^2} \right] \approx 3 \left[-\frac{\cos(QR)}{Q^2 R^2} \right]$$

$$\begin{aligned} I(Q) &= 9\Delta\rho^2 V_p^2 \left[-\frac{\cos(QR)}{Q^2 R^2} \right]^2 \\ &= 9\Delta\rho^2 V_p^2 \frac{\langle \cos^2(QR) \rangle}{Q^4 R^4} \end{aligned}$$

Porod analysis



In the short wavelength limit ($QR \gg 1$), the form factor for a sphere can be approximated

$$\mathcal{F}(Q) = 3 \left[\frac{\sin(QR)}{Q^3 R^3} - \frac{\cos(QR)}{Q^2 R^2} \right] \approx 3 \left[-\frac{\cos(QR)}{Q^2 R^2} \right]$$

$$\begin{aligned} I(Q) &= 9\Delta\rho^2 V_p^2 \left[-\frac{\cos(QR)}{Q^2 R^2} \right]^2 \\ &= 9\Delta\rho^2 V_p^2 \frac{\langle \cos^2(QR) \rangle}{Q^4 R^4} = \frac{9\Delta\rho^2 V_p^2}{Q^4 R^4} \left(\frac{1}{2} \right) \end{aligned}$$

Porod analysis



In the short wavelength limit ($QR \gg 1$), the form factor for a sphere can be approximated

$$\mathcal{F}(Q) = 3 \left[\frac{\sin(QR)}{Q^3 R^3} - \frac{\cos(QR)}{Q^2 R^2} \right] \approx 3 \left[-\frac{\cos(QR)}{Q^2 R^2} \right]$$

$$\begin{aligned} I(Q) &= 9\Delta\rho^2 V_p^2 \left[-\frac{\cos(QR)}{Q^2 R^2} \right]^2 \\ &= 9\Delta\rho^2 V_p^2 \frac{\langle \cos^2(QR) \rangle}{Q^4 R^4} = \frac{9\Delta\rho^2 V_p^2}{Q^4 R^4} \left(\frac{1}{2} \right) \end{aligned}$$

$$I(Q) = \frac{2\pi\Delta\rho^2}{Q^4} S_p$$

Porod analysis

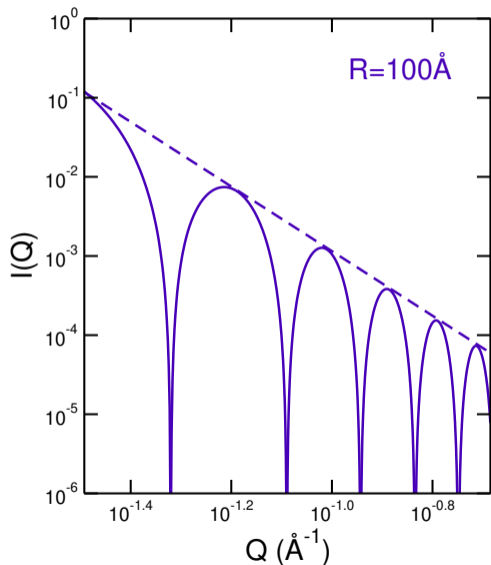


In the short wavelength limit ($QR \gg 1$), the form factor for a sphere can be approximated

$$\mathcal{F}(Q) = 3 \left[\frac{\sin(QR)}{Q^3 R^3} - \frac{\cos(QR)}{Q^2 R^2} \right] \approx 3 \left[-\frac{\cos(QR)}{Q^2 R^2} \right]$$

$$\begin{aligned} I(Q) &= 9\Delta\rho^2 V_p^2 \left[-\frac{\cos(QR)}{Q^2 R^2} \right]^2 \\ &= 9\Delta\rho^2 V_p^2 \frac{\langle \cos^2(QR) \rangle}{Q^4 R^4} = \frac{9\Delta\rho^2 V_p^2}{Q^4 R^4} \left(\frac{1}{2} \right) \end{aligned}$$

$$I(Q) = \frac{2\pi\Delta\rho^2}{Q^4} S_p$$



Porod analysis



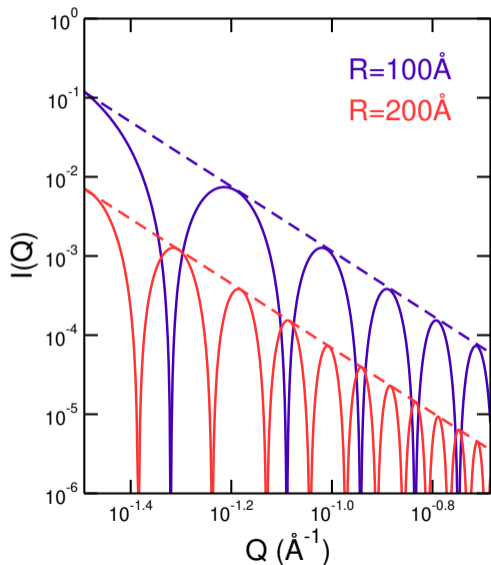
In the short wavelength limit ($QR \gg 1$), the form factor for a sphere can be approximated

$$\mathcal{F}(Q) = 3 \left[\frac{\sin(QR)}{Q^3 R^3} - \frac{\cos(QR)}{Q^2 R^2} \right] \approx 3 \left[-\frac{\cos(QR)}{Q^2 R^2} \right]$$

$$\begin{aligned} I(Q) &= 9\Delta\rho^2 V_p^2 \left[-\frac{\cos(QR)}{Q^2 R^2} \right]^2 \\ &= 9\Delta\rho^2 V_p^2 \frac{\langle \cos^2(QR) \rangle}{Q^4 R^4} = \frac{9\Delta\rho^2 V_p^2}{Q^4 R^4} \left(\frac{1}{2} \right) \end{aligned}$$

$$I(Q) = \frac{2\pi\Delta\rho^2}{Q^4} S_p$$

power law drop as Q^{-4} for spheres





Shape effect on scattering

The shape of the particle will have a significant effect on the SAXS since the form factor is derived from an integral over the particle volume, V_p .



Shape effect on scattering

The shape of the particle will have a significant effect on the SAXS since the form factor is derived from an integral over the particle volume, V_p .

If the particle is not spherical, then its “dimensionality” is not 3 and this will affect the form factor and introduce a different power law in the Porod regime.



Shape effect on scattering

The shape of the particle will have a significant effect on the SAXS since the form factor is derived from an integral over the particle volume, V_p .

If the particle is not spherical, then its “dimensionality” is not 3 and this will affect the form factor and introduce a different power law in the Porod regime.

$$\frac{dV_p}{dr} = 4\pi r^2$$

	shape	order
	sphere	



Shape effect on scattering

The shape of the particle will have a significant effect on the SAXS since the form factor is derived from an integral over the particle volume, V_p .

If the particle is not spherical, then its “dimensionality” is not 3 and this will affect the form factor and introduce a different power law in the Porod regime.

	shape	order
$dV_p = 4\pi r^2 dr$	sphere	
$dA_p = 2\pi r dr$	disk	



Shape effect on scattering

The shape of the particle will have a significant effect on the SAXS since the form factor is derived from an integral over the particle volume, V_p .

If the particle is not spherical, then its “dimensionality” is not 3 and this will affect the form factor and introduce a different power law in the Porod regime.

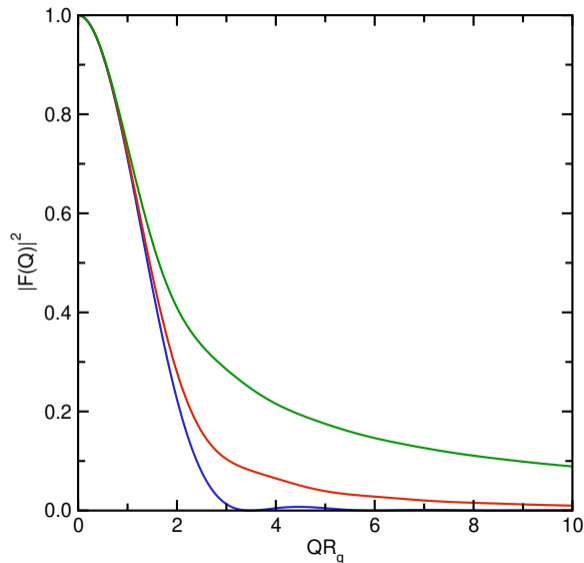
	shape	order
$dV_p = 4\pi r^2 dr$	sphere	
$dA_p = 2\pi r dr$	disk	
$dL_p = dr$	rod	



Shape effect on scattering

The shape of the particle will have a significant effect on the SAXS since the form factor is derived from an integral over the particle volume, V_p .

If the particle is not spherical, then its “dimensionality” is not 3 and this will affect the form factor and introduce a different power law in the Porod regime.



	shape	order
$dV_p = 4\pi r^2 dr$	sphere	
$dA_p = 2\pi r dr$	disk	
$dL_p = dr$	rod	

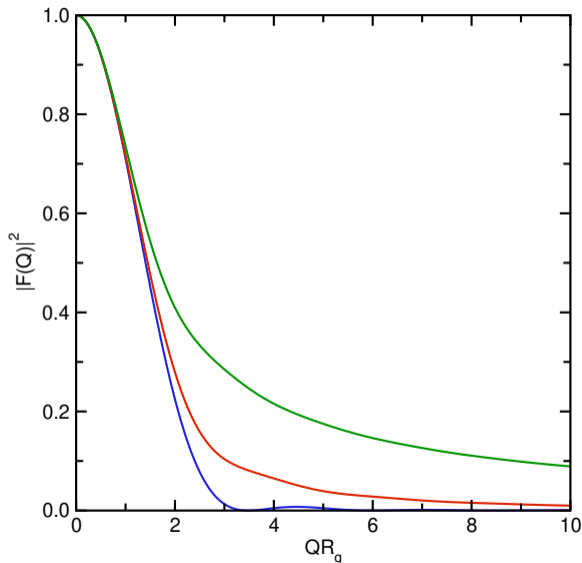


Shape effect on scattering

The shape of the particle will have a significant effect on the SAXS since the form factor is derived from an integral over the particle volume, V_p .

If the particle is not spherical, then its “dimensionality” is not 3 and this will affect the form factor and introduce a different power law in the Porod regime.

	shape	order
$dV_p = 4\pi r^2 dr$	sphere	-4
$dA_p = 2\pi r dr$	disk	
$dL_p = dr$	rod	



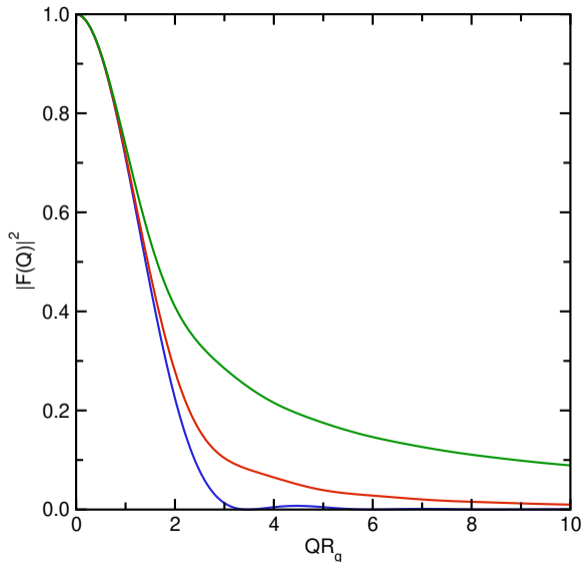


Shape effect on scattering

The shape of the particle will have a significant effect on the SAXS since the form factor is derived from an integral over the particle volume, V_p .

If the particle is not spherical, then its “dimensionality” is not 3 and this will affect the form factor and introduce a different power law in the Porod regime.

	shape	order
$dV_p = 4\pi r^2 dr$	sphere	-4
$dA_p = 2\pi r dr$	disk	-2
$dL_p = dr$	rod	-1



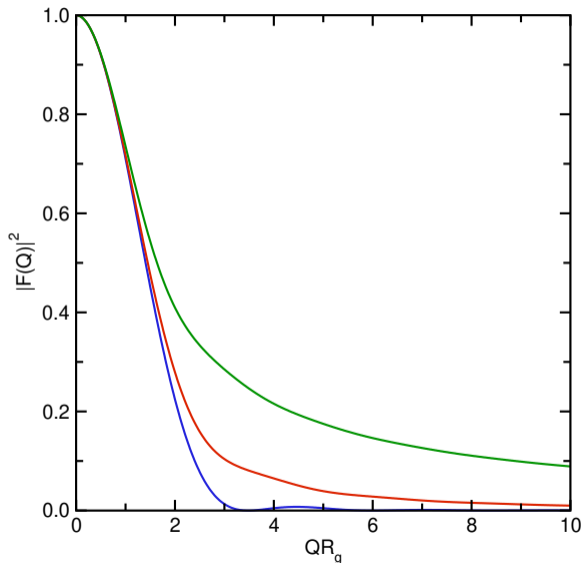


Shape effect on scattering

The shape of the particle will have a significant effect on the SAXS since the form factor is derived from an integral over the particle volume, V_p .

If the particle is not spherical, then its “dimensionality” is not 3 and this will affect the form factor and introduce a different power law in the Porod regime.

	shape	order
$dV_p = 4\pi r^2 dr$	sphere	-4
$dA_p = 2\pi r dr$	disk	-2
$dL_p = dr$	rod	-1

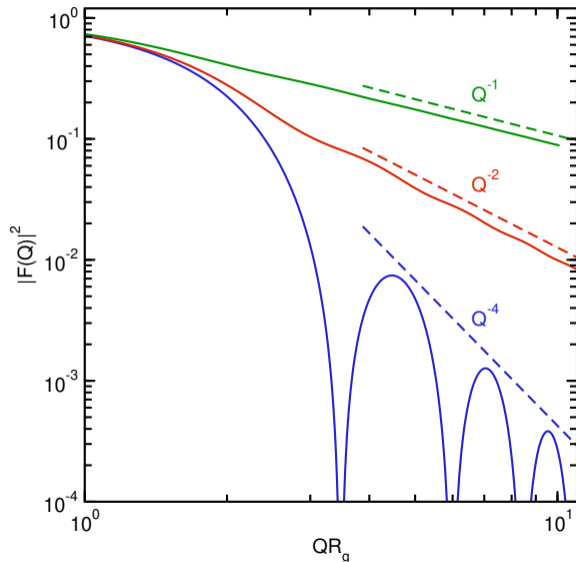




Shape effect on scattering

The shape of the particle will have a significant effect on the SAXS since the form factor is derived from an integral over the particle volume, V_p .

If the particle is not spherical, then its “dimensionality” is not 3 and this will affect the form factor and introduce a different power law in the Porod regime.



	shape	order
$dV_p = 4\pi r^2 dr$	sphere	-4
$dA_p = 2\pi r dr$	disk	-2
$dL_p = dr$	rod	-1

Polydispersivity



Analysis is simple when all particles are the same size, i.e. monodispersed and dilute,

Polydispersivity



Analysis is simple when all particles are the same size, i.e. monodispersed and dilute, more complex models must be used when the particles are polydispersed with a distribution function $D(R)$

Polydispersivity



Analysis is simple when all particles are the same size, i.e. monodispersed and dilute, more complex models must be used when the particles are polydispersed with a distribution function $D(R)$

$$I^{SAXS}(Q) = \Delta\rho^2 \int_0^\infty D(R) V_p(R)^2 |\mathcal{F}(Q, R)|^2 dR$$

Polydispersivity



Analysis is simple when all particles are the same size, i.e. monodispersed and dilute, more complex models must be used when the particles are polydispersed with a distribution function $D(R)$

$$I^{SAXS}(Q) = \Delta\rho^2 \int_0^\infty D(R) V_p(R)^2 |\mathcal{F}(Q, R)|^2 dR$$

the Schulz function is commonly used to model $D(R)$ as it goes to a delta function as the percentage polydispersivity, $p \rightarrow 0$

Polydispersivity



Analysis is simple when all particles are the same size, i.e. monodispersed and dilute, more complex models must be used when the particles are polydispersed with a distribution function $D(R)$

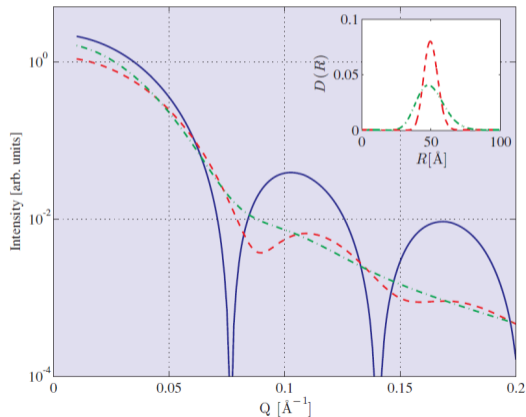
$$I^{SAXS}(Q) = \Delta\rho^2 \int_0^\infty D(R) V_p(R)^2 |\mathcal{F}(Q, R)|^2 dR$$

the Schulz function is commonly used to model $D(R)$ as it goes to a delta function as the percentage polydispersivity, $p \rightarrow 0$

$$p = 0$$

$$p = 10\%$$

$$p = 20\%$$



Unified model for SAXS



For inhomogeneous samples, using simple Guinier and Porod models can give an incorrect description of the actual sample

Unified model for SAXS



For inhomogeneous samples, using simple Guinier and Porod models can give an incorrect description of the actual sample

This can be solved, judiciously, using the Unified model proposed by Beaucage in 1995

Unified model for SAXS



For inhomogeneous samples, using simple Guinier and Porod models can give an incorrect description of the actual sample

This can be solved, judiciously, using the Unified model proposed by Beaucage in 1995

The idea is to include multiple populations each with its own Guinier dependence with R_g and a power law dependence that asymptotically approaches the Porod law for spheres

Unified model for SAXS



For inhomogeneous samples, using simple Guinier and Porod models can give an incorrect description of the actual sample

This can be solved, judiciously, using the Unified model proposed by Beaucage in 1995

The idea is to include multiple populations each with its own Guinier dependence with R_g and a power law dependence that asymptotically approaches the Porod law for spheres

$$I(q) = B_{bkg} + \sum_{i=1}^N G_i e^{-\frac{q^2 R_{g,i}^2}{3}} + e^{-\frac{q^2 R_{g,i-1}^2}{3}} B_i \left[\frac{\left(\operatorname{erf} \left\{ \frac{q R_{g,i}}{\sqrt{6}} \right\} \right)^3}{q} \right]^{P_i}$$

Unified model for SAXS



For inhomogeneous samples, using simple Guinier and Porod models can give an incorrect description of the actual sample

This can be solved, judiciously, using the Unified model proposed by Beaucage in 1995

The idea is to include multiple populations each with its own Guinier dependence with R_g and a power law dependence that asymptotically approaches the Porod law for spheres

$$I(q) = B_{bkg} + \sum_{i=1}^N G_i e^{-\frac{q^2 R_{g,i}^2}{3}} + e^{-\frac{q^2 R_{g,i-1}^2}{3}} B_i \left[\frac{\left(\operatorname{erf} \left\{ \frac{q R_{g,i}}{\sqrt{6}} \right\} \right)^3}{q} \right]^{P_i}$$

The sum is over structural levels starting with the smallest. For each level there is a Guinier exponential prefactor (G_i), a radius of gyration ($R_{g,i}$), a power law constant prefactor (B_i), and a power law exponent (P_i).



$$I(q) = B_{bkg} + \sum_{i=1}^N G_i e^{-\frac{q^2 R_{g,i}^2}{3}} + e^{-\frac{q^2 R_{g,i-1}^2}{3}} B_i \left[\frac{\left(\operatorname{erf} \left\{ \frac{q R_{g,i}}{\sqrt{6}} \right\} \right)^3}{q} \right]^{P_i}$$



$$I(q) = B_{bkg} + \sum_{i=1}^N G_i e^{-\frac{q^2 R_{g,i}^2}{3}} + e^{-\frac{q^2 R_{g,i-1}^2}{3}} B_i \left[\frac{\left(\operatorname{erf} \left\{ \frac{q R_{g,i}}{\sqrt{6}} \right\} \right)^3}{q} \right]^{P_i}$$

$R_{g,i-1}$ is the high- q power law cutoff for each level and is taken to be the radius of gyration of the previous level to avoid double counting.



$$I(q) = B_{bkg} + \sum_{i=1}^N G_i e^{-\frac{q^2 R_{g,i}^2}{3}} + e^{-\frac{q^2 R_{g,i-1}^2}{3}} B_i \left[\frac{\left(\operatorname{erf} \left\{ \frac{q R_{g,i}}{\sqrt{6}} \right\} \right)^3}{q} \right]^{P_i}$$

$R_{g,i-1}$ is the high- q power law cutoff for each level and is taken to be the radius of gyration of the previous level to avoid double counting.

Additional parameters can be added, such as a structure factor that is different than unity, and interparticle correlation parameters.



$$I(q) = B_{bkg} + \sum_{i=1}^N G_i e^{-\frac{q^2 R_{g,i}^2}{3}} + e^{-\frac{q^2 R_{g,i-1}^2}{3}} B_i \left[\frac{\left(\operatorname{erf} \left\{ \frac{q R_{g,i}}{\sqrt{6}} \right\} \right)^3}{q} \right]^{P_i}$$

$R_{g,i-1}$ is the high- q power law cutoff for each level and is taken to be the radius of gyration of the previous level to avoid double counting.

Additional parameters can be added, such as a structure factor that is different than unity, and interparticle correlation parameters.

It is important not to include more levels than are significant physically

Inter-particle interactions



Many interesting problems fall outside the dilute limit.

Inter-particle interactions



Many interesting problems fall outside the dilute limit.

In these cases, the SAXS modeling must include not only the particle form factor but an additional structure factor, $S(Q)$



Many interesting problems fall outside the dilute limit.

In these cases, the SAXS modeling must include not only the particle form factor but an additional structure factor, $S(Q)$

$$I^{SAXS}(Q) = \Delta\rho^2 V_p^2 |\mathcal{F}(\vec{Q})|^2 S(Q)$$



Many interesting problems fall outside the dilute limit.

In these cases, the SAXS modeling must include not only the particle form factor but an additional structure factor, $S(Q)$

$$I^{SAXS}(Q) = \Delta\rho^2 V_p^2 |\mathcal{F}(\vec{Q})|^2 S(Q)$$

The book has an example of this and we will look at a couple of others from recent journal articles



Many interesting problems fall outside the dilute limit.

In these cases, the SAXS modeling must include not only the particle form factor but an additional structure factor, $S(Q)$

$$I^{SAXS}(Q) = \Delta\rho^2 V_p^2 |\mathcal{F}(\vec{Q})|^2 S(Q)$$

The book has an example of this and we will look at a couple of others from recent journal articles

- SAXS of irradiated Zn nanoparticles



Many interesting problems fall outside the dilute limit.

In these cases, the SAXS modeling must include not only the particle form factor but an additional structure factor, $S(Q)$

$$I^{SAXS}(Q) = \Delta\rho^2 V_p^2 |\mathcal{F}(\vec{Q})|^2 S(Q)$$

The book has an example of this and we will look at a couple of others from recent journal articles

- SAXS of irradiated Zn nanoparticles
- Nucleation and growth of & glycine crystals

SAXS of irradiated Zn nanoparticles



Zn nanoparticles formed in SiO₂ by ion implantation irradiated with high energy Xe⁺¹⁴ ions.

"Shape elongation of embedded Zn nanoparticles induced by swift heavy ion irradiation: A SAXS study", H. Amekura, K. Kono, N. Okubo, and N. Ishikawa, *Phys. Status Solidi B* **252**, 165-169 (2015).

SAXS of irradiated Zn nanoparticles



Zn nanoparticles formed in SiO₂ by ion implantation irradiated with high energy Xe⁺¹⁴ ions.

SAXS measured with 18 keV x-rays parallel and perpendicular to the direction of irradiation.

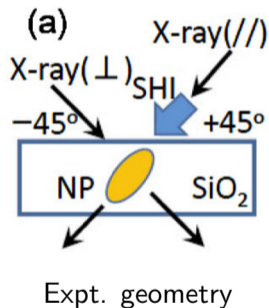
“Shape elongation of embedded Zn nanoparticles induced by swift heavy ion irradiation: A SAXS study”, H. Amekura, K. Kono, N. Okubo, and N. Ishikawa, *Phys. Status Solidi B* **252**, 165-169 (2015).

SAXS of irradiated Zn nanoparticles



Zn nanoparticles formed in SiO_2 by ion implantation irradiated with high energy Xe^{+14} ions.

SAXS measured with 18 keV x-rays parallel and perpendicular to the direction of irradiation.



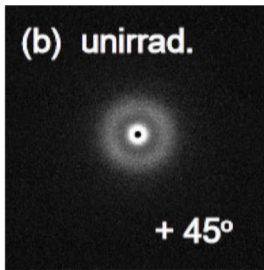
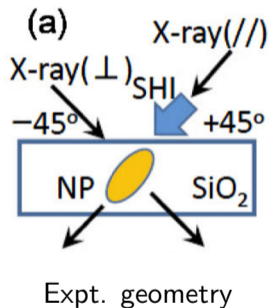
"Shape elongation of embedded Zn nanoparticles induced by swift heavy ion irradiation: A SAXS study", H. Amekura, K. Kono, N. Okubo, and N. Ishikawa, *Phys. Status Solidi B* 252, 165-169 (2015).

SAXS of irradiated Zn nanoparticles



Zn nanoparticles formed in SiO_2 by ion implantation irradiated with high energy Xe^{+14} ions.

SAXS measured with 18 keV x-rays parallel and perpendicular to the direction of irradiation.



Unirradiated

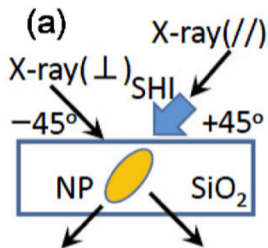
"Shape elongation of embedded Zn nanoparticles induced by swift heavy ion irradiation: A SAXS study", H. Amekura, K. Kono, N. Okubo, and N. Ishikawa, *Phys. Status Solidi B* 252, 165-169 (2015).

SAXS of irradiated Zn nanoparticles

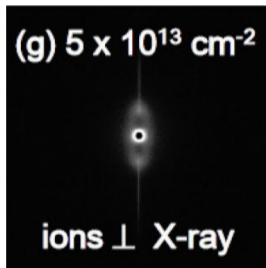


Zn nanoparticles formed in SiO₂ by ion implantation irradiated with high energy Xe⁺¹⁴ ions.

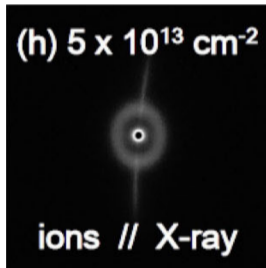
SAXS measured with 18 keV x-rays parallel and perpendicular to the direction of irradiation.



Expt. geometry



Irradiated \perp x-rays



Irradiated \parallel x-rays

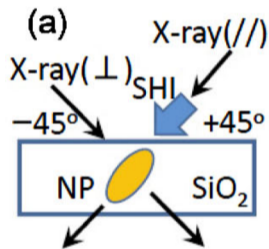
"Shape elongation of embedded Zn nanoparticles induced by swift heavy ion irradiation: A SAXS study", H. Amekura, K. Kono, N. Okubo, and N. Ishikawa, *Phys. Status Solidi B* 252, 165-169 (2015).

SAXS of irradiated Zn nanoparticles

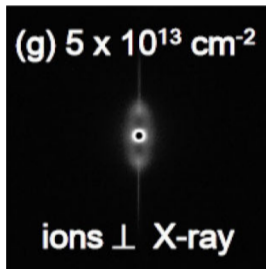


Zn nanoparticles formed in SiO₂ by ion implantation irradiated with high energy Xe⁺¹⁴ ions.

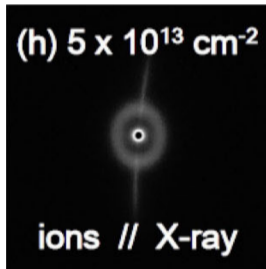
SAXS measured with 18 keV x-rays parallel and perpendicular to the direction of irradiation.



Expt. geometry



Irradiated \perp x-rays

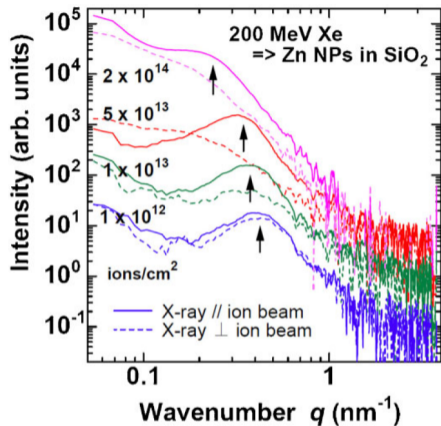


Irradiated \parallel x-rays

Straight lines from ion tracks, seen in both directions and which persist to the highest fluences.

"Shape elongation of embedded Zn nanoparticles induced by swift heavy ion irradiation: A SAXS study", H. Amekura, K. Kono, N. Okubo, and N. Ishikawa, *Phys. Status Solidi B* 252, 165-169 (2015).

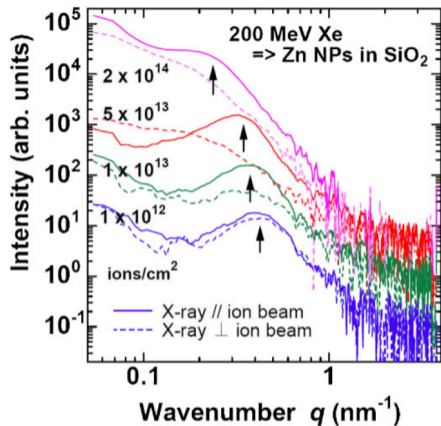
SAXS of irradiated Zn nanoparticles



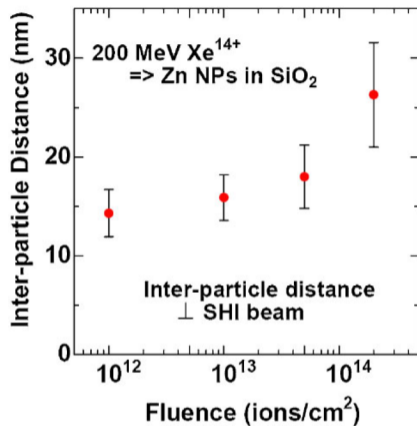
Interference peak persists for || but not ⊥ incidence

“Shape elongation of embedded Zn nanoparticles induced by swift heavy ion irradiation: A SAXS study”, H. Amekura, K. Kono, N. Okubo, and N. Ishikawa, *Phys. Status Solidi B* **252**, 165-169 (2015).

SAXS of irradiated Zn nanoparticles



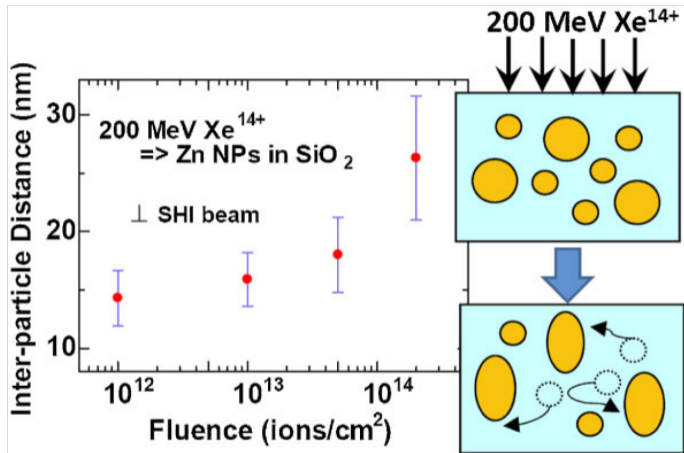
Interference peak persists for // but not ⊥ incidence



Interparticle distance increases as a function of irradiation fluence

"Shape elongation of embedded Zn nanoparticles induced by swift heavy ion irradiation: A SAXS study", H. Amekura, K. Kono, N. Okubo, and N. Ishikawa, *Phys. Status Solidi B* 252, 165-169 (2015).

SAXS of irradiated Zn nanoparticles

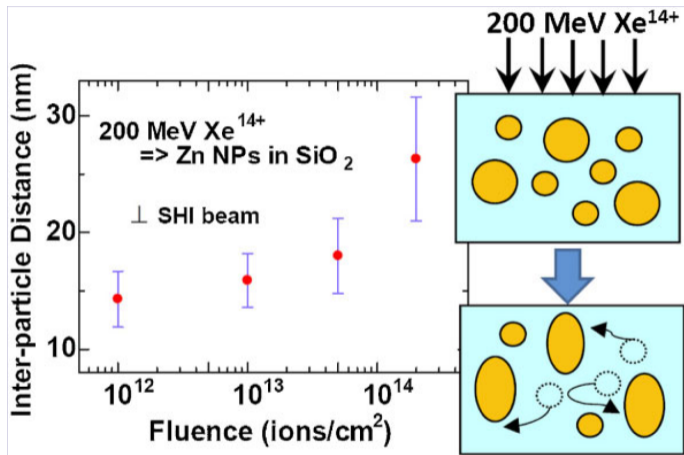


"Shape elongation of embedded Zn nanoparticles induced by swift heavy ion irradiation: A SAXS study", H. Amekura, K. Kono, N. Okubo, and N. Ishikawa, *Phys. Status Solidi B* 252, 165-169 (2015).

SAXS of irradiated Zn nanoparticles



Growth of interparticle spacing is due to dissolution and re-agglomeration with fluence leading to larger interparticle spacings



"Shape elongation of embedded Zn nanoparticles induced by swift heavy ion irradiation: A SAXS study", H. Amekura, K. Kono, N. Okubo, and N. Ishikawa, *Phys. Status Solidi B* 252, 165-169 (2015).

Nucleation & growth of glycine



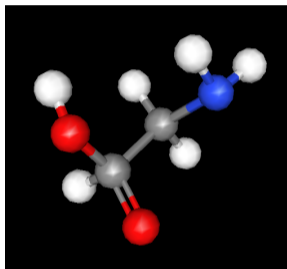
Can SAXS help us understand the nucleation and growth of a simple molecule which is the prototype for pharmaceutical compounds?

"SAXS study of the nucleation of glycine crystals from a supersaturated solution," S. Chattopadhyay et al. *Crystal Growth Design* **5**, 523-527 (2004)

Nucleation & growth of glycine



Can SAXS help us understand the nucleation and growth of a simple molecule which is the prototype for pharmaceutical compounds?

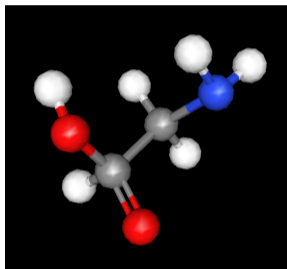


"SAXS study of the nucleation of glycine crystals from a supersaturated solution," S. Chattopadhyay et al. *Crystal Growth Design* **5**, 523-527 (2004)

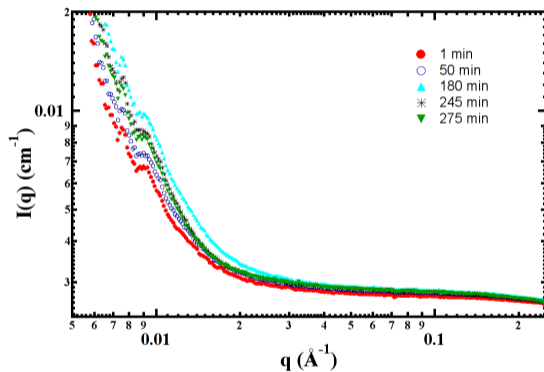
Nucleation & growth of glycine



Can SAXS help us understand the nucleation and growth of a simple molecule which is the prototype for pharmaceutical compounds?



Initial studies at 12keV observe change in R_g upon crystallization.

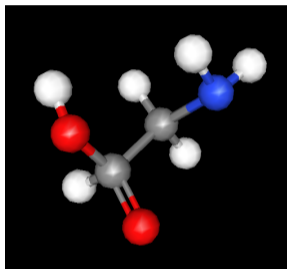


"SAXS study of the nucleation of glycine crystals from a supersaturated solution," S. Chattopadhyay et al. *Crystal Growth Design* 5, 523-527 (2004)

Nucleation & growth of glycine

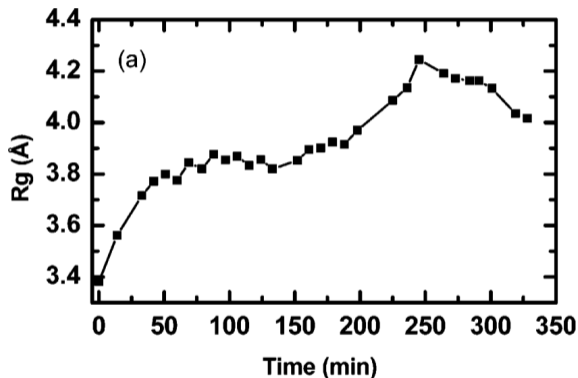


Can SAXS help us understand the nucleation and growth of a simple molecule which is the prototype for pharmaceutical compounds?



Initial studies at 12keV observe change in R_g upon crystallization.

Results confirm a two-step model of crystallization and dimerization in aqueous solution.

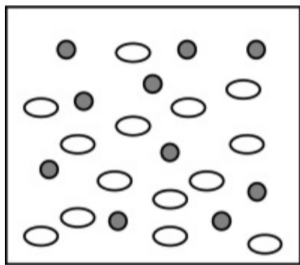


"SAXS study of the nucleation of glycine crystals from a supersaturated solution," S. Chattopadhyay et al. *Crystal Growth Design* 5, 523-527 (2004)

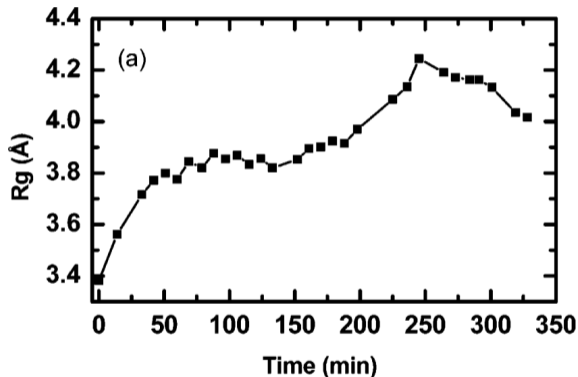
Nucleation & growth of glycine



Can SAXS help us understand the nucleation and growth of a simple molecule which is the prototype for pharmaceutical compounds?



Initial studies at 12keV observe change in R_g upon crystallization.



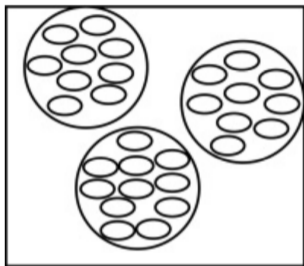
Results confirm a two-step model of crystallization and dimerization in aqueous solution.

"SAXS study of the nucleation of glycine crystals from a supersaturated solution," S. Chattopadhyay et al. *Crystal Growth Design* 5, 523-527 (2004)

Nucleation & growth of glycine

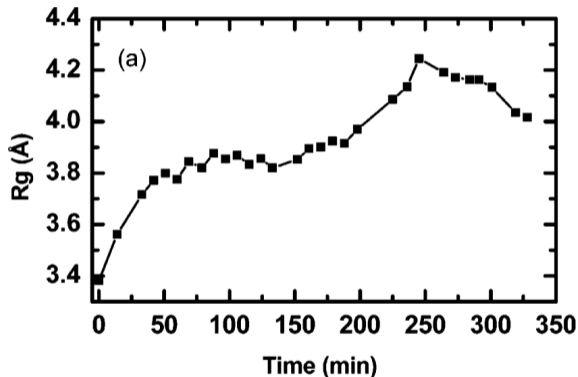


Can SAXS help us understand the nucleation and growth of a simple molecule which is the prototype for pharmaceutical compounds?



Initial studies at 12keV observe change in R_g upon crystallization.

Results confirm a two-step model of crystallization and dimerization in aqueous solution.

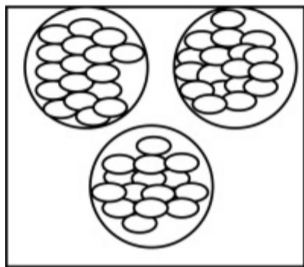


"SAXS study of the nucleation of glycine crystals from a supersaturated solution," S. Chattopadhyay et al. *Crystal Growth Design* 5, 523-527 (2004)

Nucleation & growth of glycine

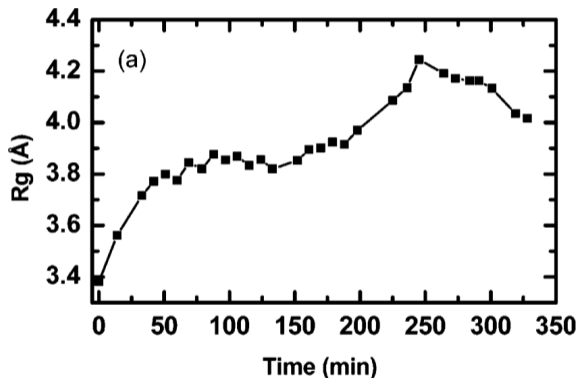


Can SAXS help us understand the nucleation and growth of a simple molecule which is the prototype for pharmaceutical compounds?



Initial studies at 12keV observe change in R_g upon crystallization.

Results confirm a two-step model of crystallization and dimerization in aqueous solution.



"SAXS study of the nucleation of glycine crystals from a supersaturated solution," S. Chattopadhyay et al. *Crystal Growth Design* 5, 523-527 (2004)

Glycine nucleation



Long nucleation times due to heating from absorbed 12 keV x-rays.

Glycine nucleation



Long nucleation times due to heating from absorbed 12 keV x-rays.

Change to 25 keV x-rays reduces crystallization time to under 90 min

Glycine nucleation

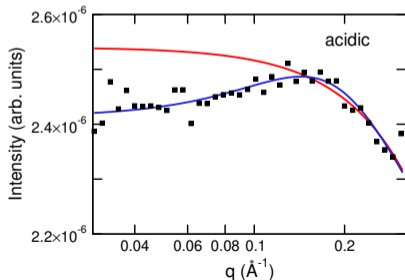
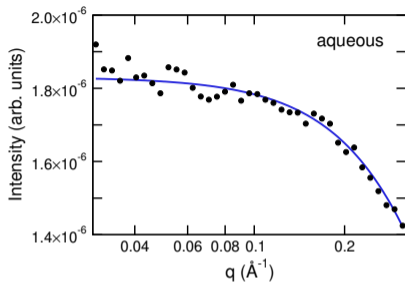


Long nucleation times due to heating from absorbed 12 keV x-rays.

Change to 25 keV x-rays reduces crystallization time to under 90 min

Different polymorphs are produced under varying conditions so study extended to both neutral and acidic solutions

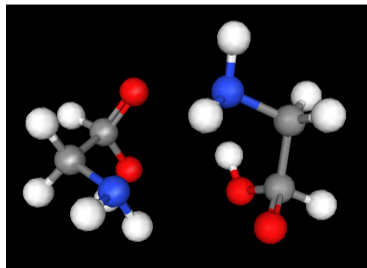
Glycine nucleation



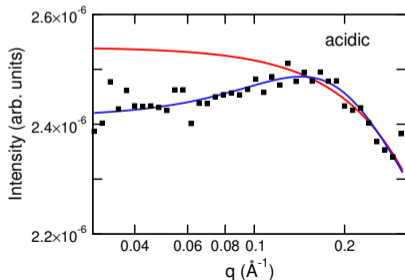
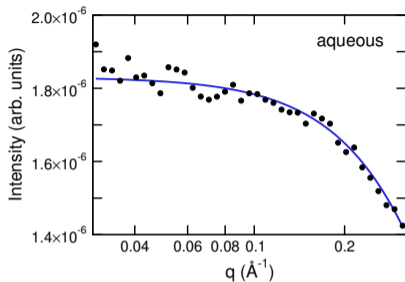
Long nucleation times due to heating from absorbed 12 keV x-rays.

Change to 25 keV x-rays reduces crystallization time to under 90 min

Different polymorphs are produced under varying conditions so study extended to both neutral and acidic solutions



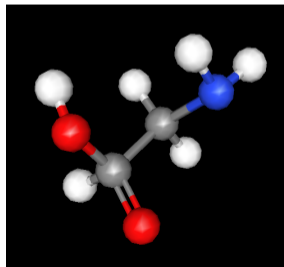
Glycine nucleation

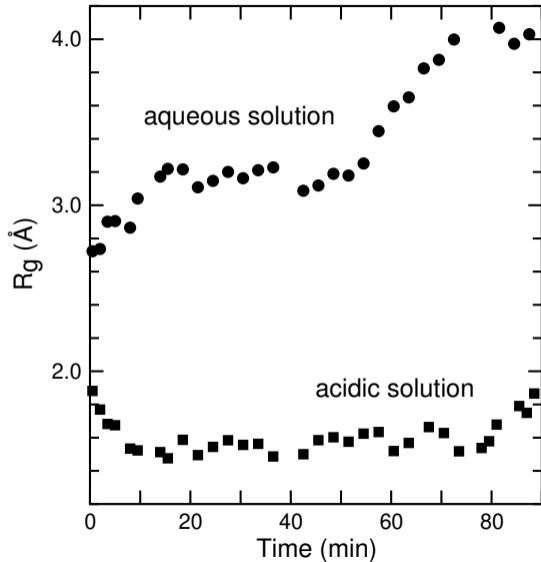


Long nucleation times due to heating from absorbed 12 keV x-rays.

Change to 25 keV x-rays reduces crystallization time to under 90 min

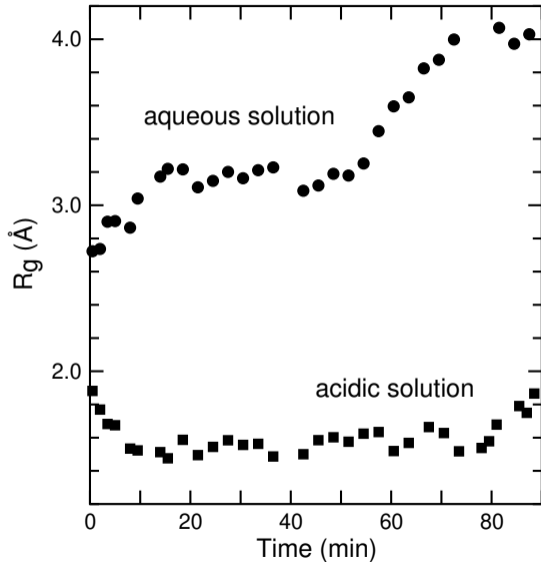
Different polymorphs are produced under varying conditions so study extended to both neutral and acidic solutions





In aqueous solution, R_g implies dimerization and increases due to aggregation until crystallization

“Relationship between self-association of glycine molecules in supersaturated solution and solid state outcome”,
D. Erdemir et al. *Phys. Rev. Lett.* **99**, 115702 (2007)



In aqueous solution, R_g implies dimerization and increases due to aggregation until crystallization

In acidic solution, R_g remains small and implies that no dimerization or aggregation occurs before nucleation

“Relationship between self-association of glycine molecules in supersaturated solution and solid state outcome”,
D. Erdemir et al. *Phys. Rev. Lett.* **99**, 115702 (2007)

Size exclusion chromatography SAXS



SAXS of biological molecules is an excellent way of getting some information about the molecules as they exist in solution.

Size exclusion chromatography SAXS



SAXS of biological molecules is an excellent way of getting some information about the molecules as they exist in solution.

Obtaining information about R_g and the Porod region, combined with modeling and the known crystallographic structures can give a more complete picture of how these molecules function.

Size exclusion chromatography SAXS



SAXS of biological molecules is an excellent way of getting some information about the molecules as they exist in solution.

Obtaining information about R_g and the Porod region, combined with modeling and the known crystallographic structures can give a more complete picture of how these molecules function.

A major problem in these systems is aggregation and impurities. Pre-purification of samples is important but if they are left for some time before the SAXS measurement is performed, there can be decomposition.

Size exclusion chromatography SAXS



SAXS of biological molecules is an excellent way of getting some information about the molecules as they exist in solution.

Obtaining information about R_g and the Porod region, combined with modeling and the known crystallographic structures can give a more complete picture of how these molecules function.

A major problem in these systems is aggregation and impurities. Pre-purification of samples is important but if they are left for some time before the SAXS measurement is performed, there can be decomposition.

Even without any aggregation or decomposition, separation into a monodisperse molecule size is challenging.

Size exclusion chromatography SAXS



SAXS of biological molecules is an excellent way of getting some information about the molecules as they exist in solution.

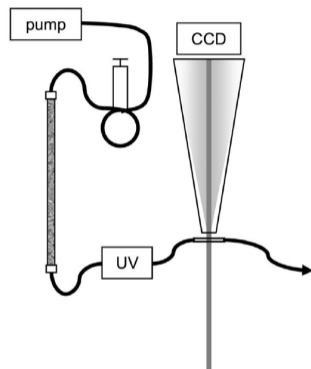
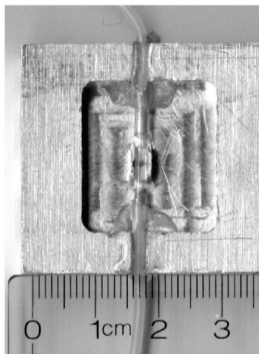
Obtaining information about R_g and the Porod region, combined with modeling and the known crystallographic structures can give a more complete picture of how these molecules function.

A major problem in these systems is aggregation and impurities. Pre-purification of samples is important but if they are left for some time before the SAXS measurement is performed, there can be decomposition.

Even without any aggregation or decomposition, separation into a monodisperse molecule size is challenging.

Mathew, Mirza & Menhart, "Liquid-chromatography-coupled SAXS for accurate sizing of aggregating proteins," *J. Synchrotron Rad.* **11**, 314-318 (2004) developed a technique which is now being used routinely in biological SAXS, called Size Exclusion Chromatography SAXS.

Size exclusion chromatography SAXS

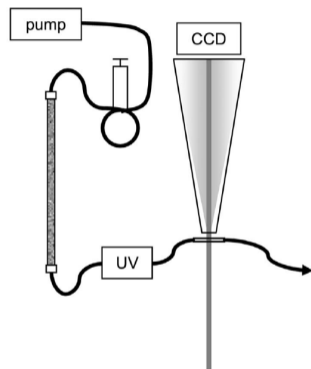
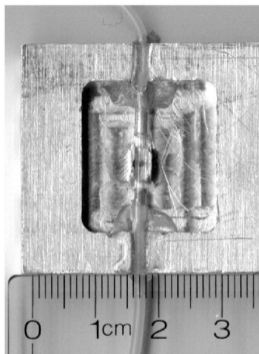


"Liquid-chromatography-coupled SAXS for accurate sizing of aggregating proteins," Mathew, Mirza & Menhart, *J. Synchrotron Rad.* **11**, 314-318 (2004).

Size exclusion chromatography SAXS



2m SAXS camera, 1.03\AA (12 keV) x-rays were used



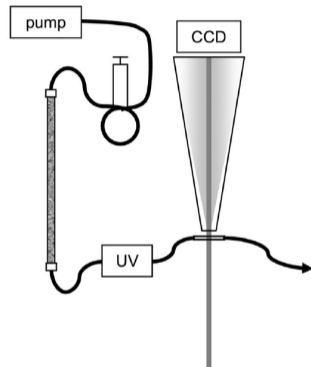
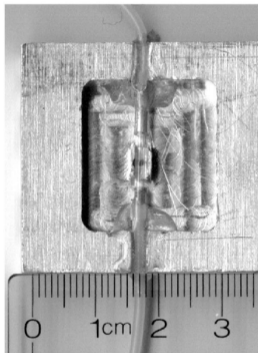
"Liquid-chromatography-coupled SAXS for accurate sizing of aggregating proteins," Mathew, Mirza & Menhart, *J. Synchrotron Rad.* **11**, 314-318 (2004).

Size exclusion chromatography SAXS



2m SAXS camera, 1.03\AA (12 keV) x-rays were used

2s exposure times every 20s, with 0.25 ml/min flow rate



"Liquid-chromatography-coupled SAXS for accurate sizing of aggregating proteins," Mathew, Mirza & Menhart, *J. Synchrotron Rad.* **11**, 314-318 (2004).

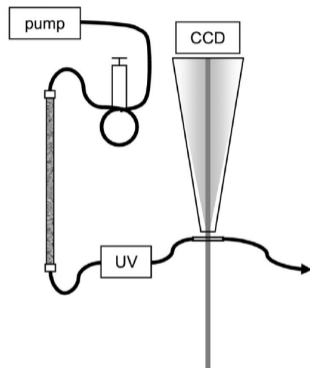
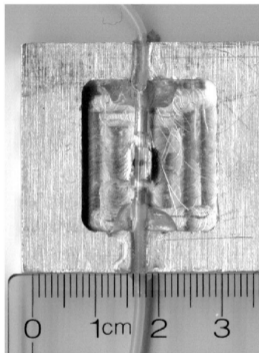
Size exclusion chromatography SAXS



2m SAXS camera, 1.03\AA (12 keV) x-rays were used

2s exposure times every 20s, with 0.25 ml/min flow rate

samples of (1) cytochrome c, (2) plasminogen, (3) mixture of cytochrome c bovine serum albumin, and blue dextran



"Liquid-chromatography-coupled SAXS for accurate sizing of aggregating proteins," Mathew, Mirza & Menhart, *J. Synchrotron Rad.* **11**, 314-318 (2004).

Size exclusion chromatography SAXS

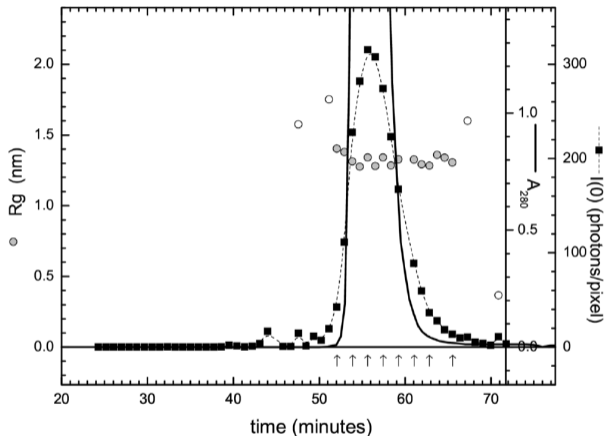


2m SAXS camera, 1.03\AA (12 keV) x-rays were used

2s exposure times every 20s, with 0.25 ml/min flow rate

samples of (1) cytochrome c, (2) plasminogen, (3) mixture of cytochrome c bovine serum albumin, and blue dextran

for cytochrome c, forward scatter (black squares) measures the total number of electrons in the beam



"Liquid-chromatography-coupled SAXS for accurate sizing of aggregating proteins," Mathew, Mirza & Menhart, *J. Synchrotron Rad.* **11**, 314-318 (2004).

Size exclusion chromatography SAXS

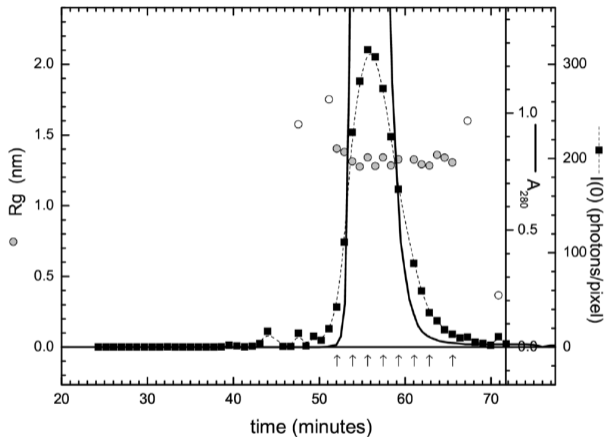


2m SAXS camera, 1.03\AA (12 keV) x-rays were used

2s exposure times every 20s, with 0.25 ml/min flow rate

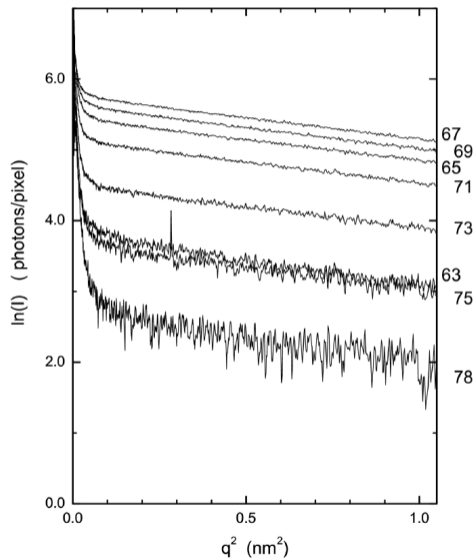
samples of (1) cytochrome c, (2) plasminogen, (3) mixture of cytochrome c bovine serum albumin, and blue dextran

for cytochrome c, forward scatter (black squares) measures the total number of electrons in the beam R_g is constant throughout the main peak



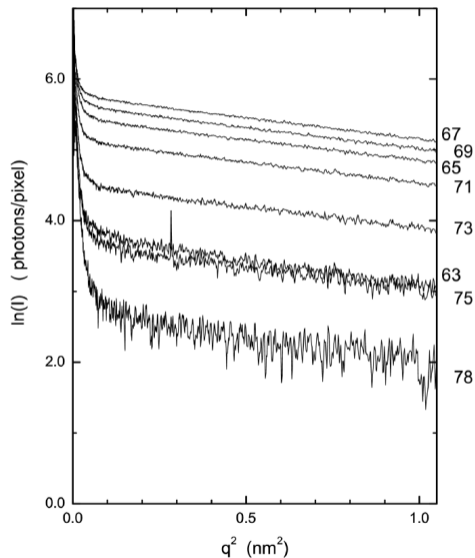
"Liquid-chromatography-coupled SAXS for accurate sizing of aggregating proteins," Mathew, Mirza & Menhart, *J. Synchrotron Rad.* **11**, 314-318 (2004).

Cytochrome c - Guinier plots



"Liquid-chromatography-coupled SAXS for accurate sizing of aggregating proteins," Mathew, Mirza & Menhart, *J. Synchrotron Rad.* **11**, 314-318 (2004).

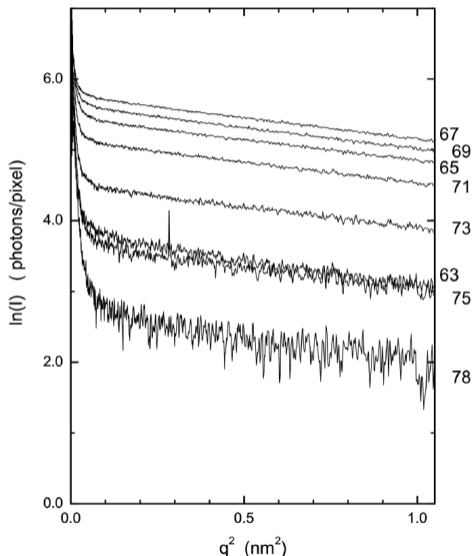
Cytochrome c - Guinier plots



Plot from times marked with arrows on R_g plot.

"Liquid-chromatography-coupled SAXS for accurate sizing of aggregating proteins," Mathew, Mirza & Menhart, *J. Synchrotron Rad.* **11**, 314-318 (2004).

Cytochrome c - Guinier plots

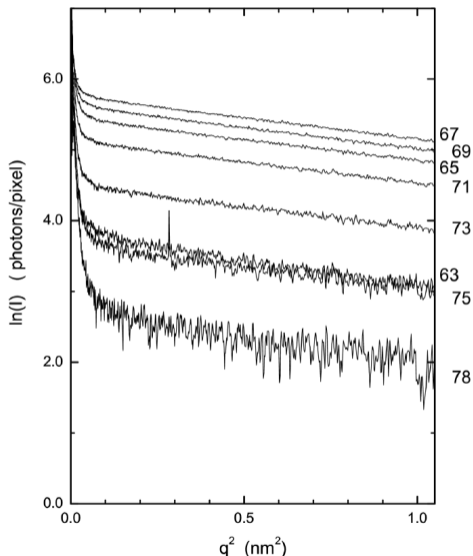


Plot from times marked with arrows on R_g plot.

Guinier plots are parallel, indicating a single species present (a single critical exponent).

"Liquid-chromatography-coupled SAXS for accurate sizing of aggregating proteins," Mathew, Mirza & Menhart, *J. Synchrotron Rad.* **11**, 314-318 (2004).

Cytochrome c - Guinier plots



Plot from times marked with arrows on R_g plot.

Guinier plots are parallel, indicating a single species present (a single critical exponent).

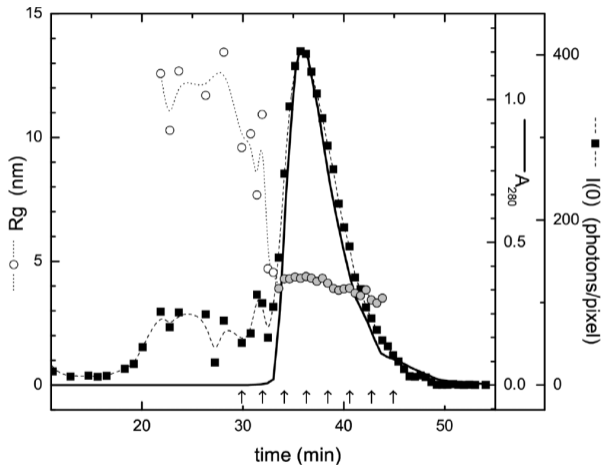
Even lowest intensity data set gives a consistent R_g .

"Liquid-chromatography-coupled SAXS for accurate sizing of aggregating proteins," Mathew, Mirza & Menhart, *J. Synchrotron Rad.* **11**, 314-318 (2004).

Plasminogen & 3-component mixture



Constant R_g in region where $A_{UV}/I(0)$ is constant.

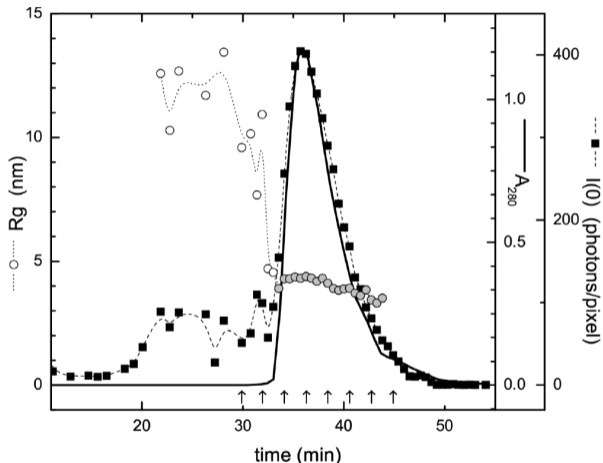


"Liquid-chromatography-coupled SAXS for accurate sizing of aggregating proteins," Mathew, Mirza & Menhart, *J. Synchrotron Rad.* **11**, 314-318 (2004).

Plasminogen & 3-component mixture



Constant R_g in region where $A_{UV}/I(0)$ is constant. Aggregates precede the main peak and show wildly varying R_g .



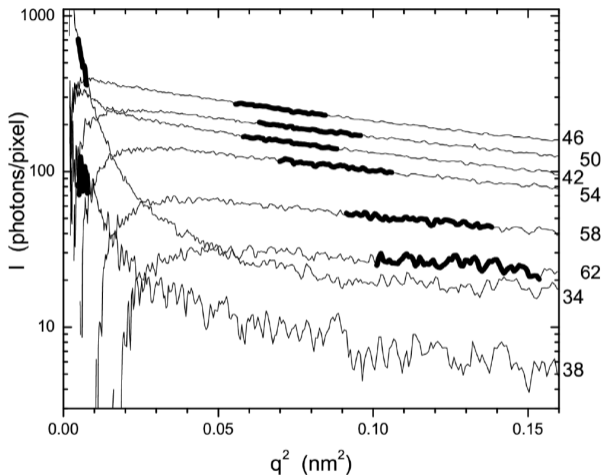
"Liquid-chromatography-coupled SAXS for accurate sizing of aggregating proteins," Mathew, Mirza & Menhart, *J. Synchrotron Rad.* **11**, 314-318 (2004).

Plasminogen & 3-component mixture



Constant R_g in region where $A_{UV}/I(0)$ is constant. Aggregates precede the main peak and show wildly varying R_g .

Guinier plots labeled 34 and 38 show presence of aggregates and the slopes are not parallel, indicating multiple sized species



"Liquid-chromatography-coupled SAXS for accurate sizing of aggregating proteins," Mathew, Mirza & Menhart, *J. Synchrotron Rad.* **11**, 314-318 (2004).

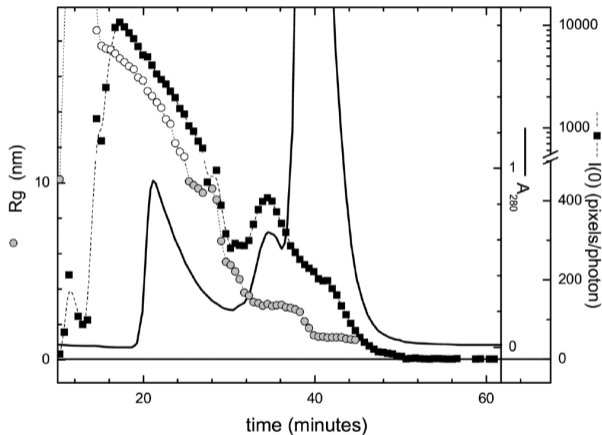
Plasminogen & 3-component mixture



Constant R_g in region where $A_{UV}/I(0)$ is constant. Aggregates precede the main peak and show wildly varying R_g .

Guinier plots labeled 34 and 38 show presence of aggregates and the slopes are not parallel, indicating multiple sized species

The three components show consistent R_g and can be individually identified despite the overlap.



"Liquid-chromatography-coupled SAXS for accurate sizing of aggregating proteins," Mathew, Mirza & Menhart, *J. Synchrotron Rad.* **11**, 314-318 (2004).

Porosity in CaO calcination



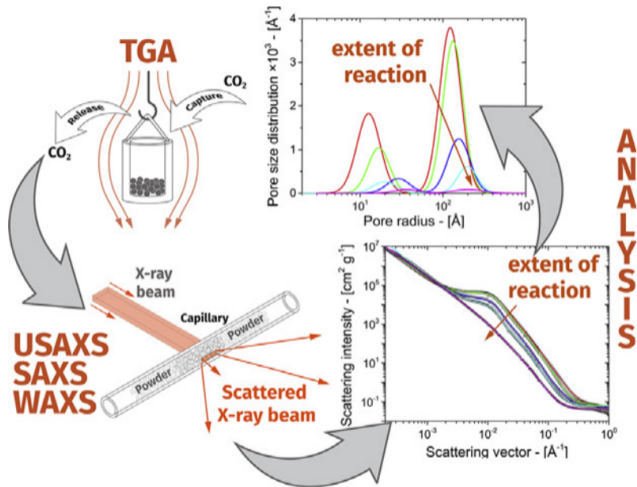
SAXS was used to study the nature of the porosity and particle sizes of CaO obtained by calcining CaCO₃.

"Analysis of textural properties of CaO-based CO₂ sorbents by ex-situ USAXS," A. Benedetti, J. Ilavsky, C.U. Segre, and M. Strumendo, *Chem. Eng. J.* **355**, 760-776 (2019).

Porosity in CaO calcination



SAXS was used to study the nature of the porosity and particle sizes of CaO obtained by calcining CaCO₃.



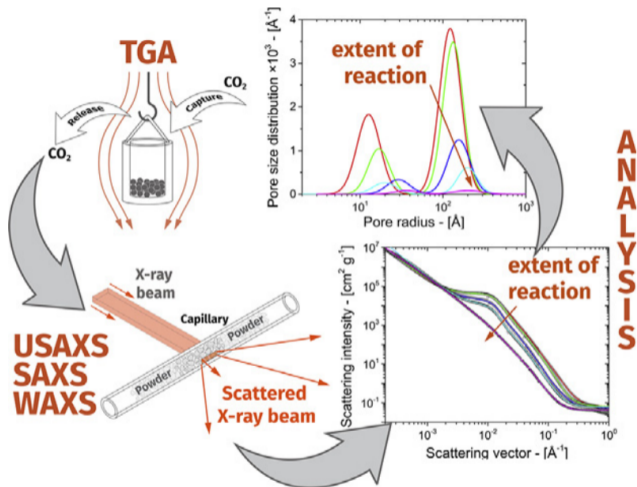
"Analysis of textural properties of CaO-based CO₂ sorbents by ex-situ USAXS," A. Benedetti, J. Ilavsky, C.U. Segre, and M. Strumendo, *Chem. Eng. J.* **355**, 760-776 (2019).

Porosity in CaO calcination



SAXS was used to study the nature of the porosity and particle sizes of CaO obtained by calcining CaCO_3 .

CaO can be used for carbon capture and then recycled by calcination. It is important to understand the meso structure of the material at different stages of the process



"Analysis of textural properties of CaO-based CO_2 sorbents by ex-situ USAXS," A. Benedetti, J. Ilavsky, C.U. Segre, and M. Strumendo, *Chem. Eng. J.* **355**, 760-776 (2019).

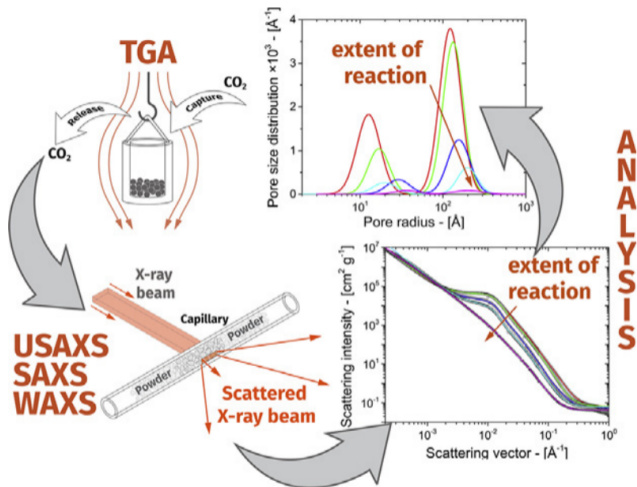
Porosity in CaO calcination



SAXS was used to study the nature of the porosity and particle sizes of CaO obtained by calcining CaCO₃.

CaO can be used for carbon capture and then recycled by calcination. It is important to understand the meso structure of the material at different stages of the process

The samples were studied ex-situ at Sector 9-ID using USAXS and analyzed with a unified fit model

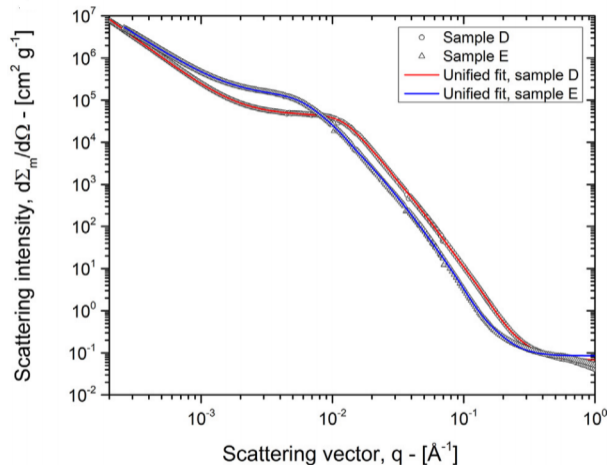


"Analysis of textural properties of CaO-based CO₂ sorbents by ex-situ USAXS," A. Benedetti, J. Ilavsky, C.U. Segre, and M. Strumendo, *Chem. Eng. J.* **355**, 760-776 (2019).

Porosity in CaO calcination



Sample D was calcined at 900 °C for 50 minutes while sample E was calcined at the same temperature for 240 minutes



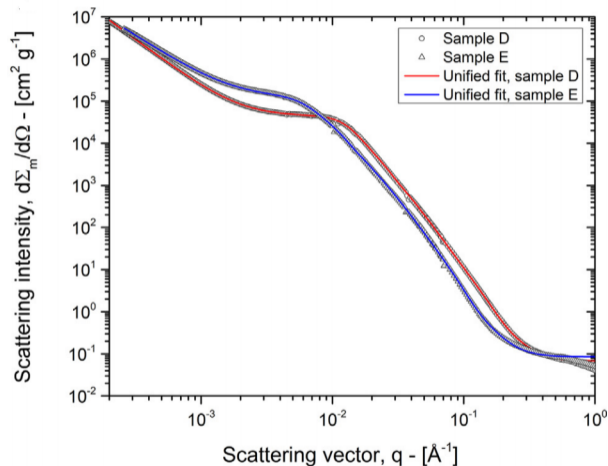
"Analysis of textural properties of CaO-based CO₂ sorbents by ex-situ USAXS," A. Benedetti, J. Ilavsky, C.U. Segre, and M. Strumendo, *Chem. Eng. J.* **355**, 760-776 (2019).

Porosity in CaO calcination



Sample D was calcined at 900 °C for 50 minutes while sample E was calcined at the same temperature for 240 minutes

The SAXS shows the grain growth evolution between the two samples and it is clear that the samples need a multilevel unified fit

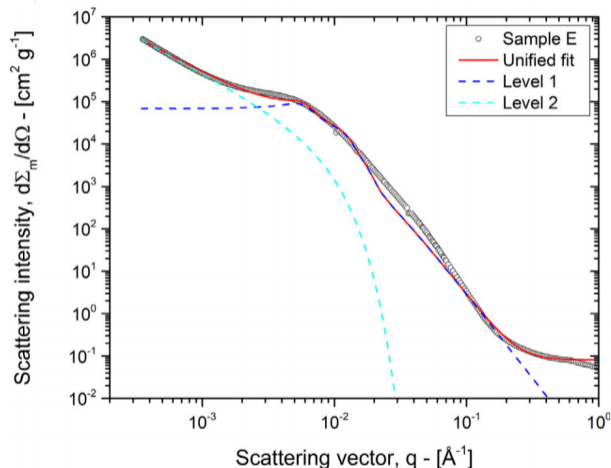


"Analysis of textural properties of CaO-based CO₂ sorbents by ex-situ USAXS," A. Benedetti, J. Ilavsky, C.U. Segre, and M. Strumendo, *Chem. Eng. J.* **355**, 760-776 (2019).

Porosity in CaO calcination



The components of the unified fit model are shown for a two level fit and it is clear that 2 levels are insufficient.



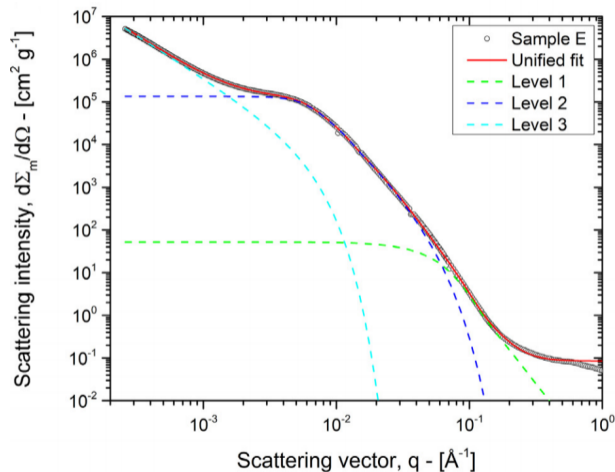
"Analysis of textural properties of CaO-based CO_2 sorbents by ex-situ USAXS," A. Benedetti, J. Ilavsky, C.U. Segre, and M. Strumendo, *Chem. Eng. J.* **355**, 760-776 (2019).

Porosity in CaO calcination



The components of the unified fit model are shown for a two level fit and it is clear that 2 levels are insufficient.

A three level fit works well for the calcined samples and from this one can extract the pore sizes for two different pore populations in the calcined samples

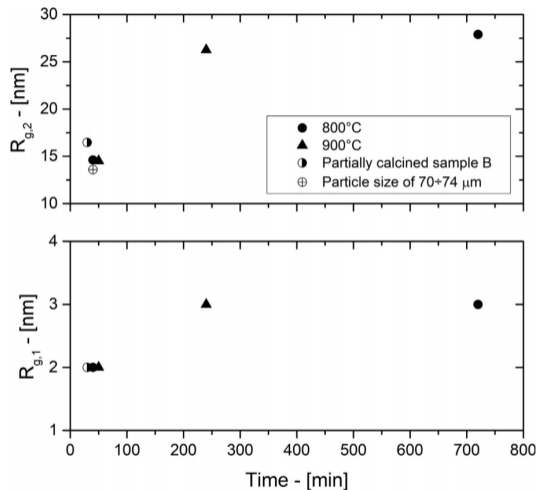


"Analysis of textural properties of CaO-based CO₂ sorbents by ex-situ USAXS," A. Benedetti, J. Ilavsky, C.U. Segre, and M. Strumendo, *Chem. Eng. J.* **355**, 760-776 (2019).

Porosity in CaO calcination



Fitting a series of samples calcined at varying temperatures and times shows the evolution of the radii of gyration of the two populations corresponding to the pore sizes



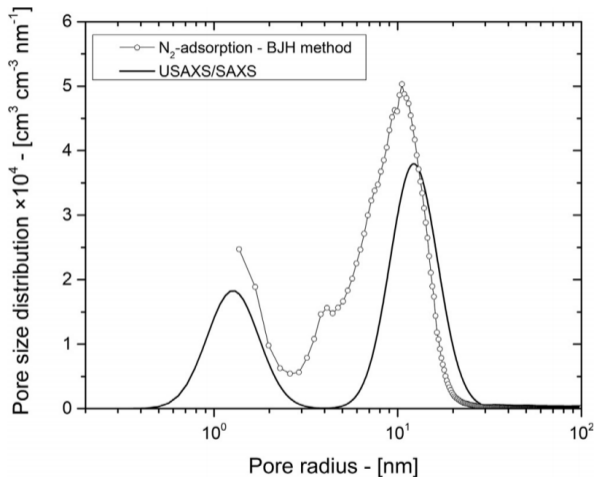
"Analysis of textural properties of CaO-based CO₂ sorbents by ex-situ USAXS," A. Benedetti, J. Ilavsky, C.U. Segre, and M. Strumendo, *Chem. Eng. J.* **355**, 760-776 (2019).

Porosity in CaO calcination



Fitting a series of samples calcined at varying temperatures and times shows the evolution of the radii of gyration of the two populations corresponding to the pore sizes

The resulting pore size distributions correspond well to those measured using gas adsorption methods



"Analysis of textural properties of CaO-based CO_2 sorbents by ex-situ USAXS," A. Benedetti, J. Ilavsky, C.U. Segre, and M. Strumendo, *Chem. Eng. J.* **355**, 760-776 (2019).